Düzce University Journal of Science & Technology

Research Article

Grid Connected Inverter

Fatih EVRAN [a,*]

[a] *Elektrik-Elektronik Mühendisliği Bölümü, Mühendislik Fakültesi, Düzce Üniversitesi, Düzce, TÜRKİYE*
** Sorumlu yazarın e-posta adresi: fatihevran@duzce.edu.tr*

ABSTRACT

This paper presents solar based single phase grid connected inverter system. In such a system, DC-DC converter is both used to boost low PV panel voltage and ensures that the solar panel operates at maximum power while Full bridge inverter injects the maximum power from the solar panel to the grid. The system is reliable because it does not cause control complexity and also it is preferred to obtain a low THD (Total harmonic distortion). But, the main disadvantages of the converters such as a boost or a flyback type are limited voltage gain and low efficiency. In the proposed topology, the DC-DC converter with galvanic insulation and high voltage gain characteristics can connect a low-voltage solar panel to the grid. Simulation results are given for the system which inverts MPPT voltage range of 20-30 V DC to grid voltage of 220 V(rms) at power range of 60-300 W with a unity power factor.

Keywords: *Inverter, Step up converter, Maximum power point track, Solar panel*

Şebeke Bağlantılı Evirici

ÖZET

Bu çalışma, tek fazlı şebekeye bağlı güneş paneli uygulamaları için bir evirici topolojisini sunmaktadır. Böyle bir sistemde, Tam köprü eviricisi güneş panelinden elektrik şebekesine maksimum güç verirken, DA-DA dönüştürücüsü hem düşük PV panel gerilimini arttırmak hem de güneş panelinin maksimum güçte çalışmasını sağlamak için kullanılmaktadır. Sistem, denetim karmaşıklığına neden olmadığından güvenilirdir ve düşük bir THB (Toplam harmonik bozulma)'si olduğundan dolayı tercih edilmektedir. Buna karşın, Boost ve Flyback gibi dönüştürücülerin ana olumsuzlukları sınırlı gerilim kazancına ve düşük verime sahip olmasıdır. Önerilen topolojide, galvanik yalıtımlı ve yüksek gerilim kazançlı DA-DA dönüştürücüsü, düşük gerilimli güneş panelini elektrik şebekesine bağlayabilmektedir. Benzetim sonuçları, 60-300 W'lık güç aralığında,20-30V MPPT gerilim aralığını, 220 V (rms) şebeke gerilimine birim güç faktörü ile çeviren sistem için verilmiştir

Anahtar Kelimeler: *Evirici, DA-DA dönüştürücü, Maksimum güç nokta izleyicisi, Güneş panel*

Received: 13/11/2017, Revised: 19/02/2018, Accepted: 21/02/2018

I. INTRODUCTION

In recent decades, solar, wind and fuel cell technologies as alternative energy sources have widely been developed because of environment population. Especially, solar energy which is an important source of renewable energy is used intensively in world thanks to decreasing costs. On the other hand, the output voltage of the PV (photovoltaic) panels is too low to be connected to grid. For instance, it has MPPT (maximum power point track) voltage range of 20-30 V at power range of 60-300 W. So, PV panels can be connected in series to obtain higher output voltage. But, to connect multiple PV panels cause a low MPPT efficiency because of partial shading. The problem can be prevented by performing individual MPPT for each panel. This increases MPPT efficiency in the topology known as AC module [1-4]. Recently, The AC module topology is divided into three classes with transformerless isolation [5-9], with low frequency transformer [10] and with high frequency transformer [11-20]. Due to security reasons and electrical noise, isolation transformer is preferred. But, due to bulky and expensive, the grid frequency transformer is not suitable. According to dc link configurations, the topologies with high frequency transformer can be classified into three different configurations. In the first configuration, DC-DC stage generates rectified sinusoidal output and the inverter unfolds the output [11-16]. Although the configuration reduces switching devices, there is a fluctuation in the input current at twice the frequency of the grid and MPPT efficiency is decreased.

The second configuration utilizes DC/AC inverter and AC/AC converter without dc link [17, 18]. But, it needs more witches. The third configuration performs high step up converter and inverter with a constant DC link [19, 20]. MPPT efficiency is high thanks to the low input current ripple.

Recently, Z-source inverter topologies have been widely reported for various applications in the literature [9, 21-23]. This paper presents the inverter topology which consists of an isolated DC-AC full-bridge and a Z source based DC–DC converter with high voltage gain for AC module applications. The proposed circuit configuration is shown in Fig. 1. The DC-DC converter interfaces to the PV panel and regulates a constant DC link voltage. Also, the converter is used to track the MPPT. The full bridge inverter converts the constant DC voltage into sinusoid AC voltage with a unity power factor.

The organization of the paper is as follows: Section II discusses the operation principle of converter. In Section III, PV module characteristic analysis is given. In Section IV, simulation results are provided for the system which inverts MPPT voltage range of 20-30 V DC to grid voltage of 220 V(rms) at power range of 60-300 W with a unity power factor. Conclusions are given in Section V.

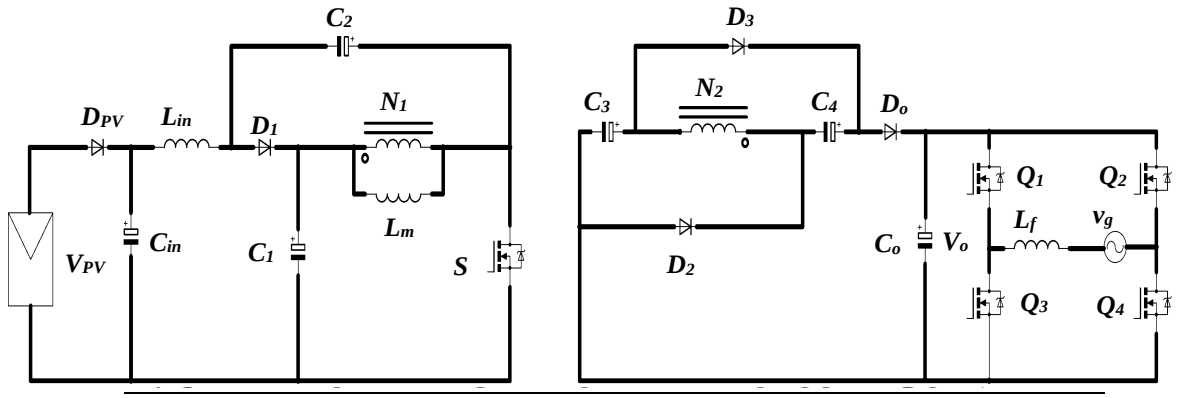

Figure 1. *The proposed grid-connected single-phase inverter* structure

The converter circuit is shown in Fig. 2. Coupled inductors are presented by a magnetizing inductor (L_m) and an ideal transformer by neglecting leakage inductors. The circuit employs 5 capacitors (C_o, C_1, C_2, C_3, C_4), and 4 diodes (D_o, D_1, D_2, D_3). S is the main power switch. L_1 is the primary inductance and L_2 is the secondary inductance. N_1 and N_2 are the *number of turns* on the primary and the secondary windings of the transformer, respectively. When S is turned on, the diodes D_1, D_2 and D_3 are turned off while D_o conducts and the capacitors C_3 and C_4 are discharged through load. When S is turned off, D_1 starts conducting and the inductor currents i_{L1} and i_{L2} flow through the capacitors C_2, C_3 and C_4, respectively.

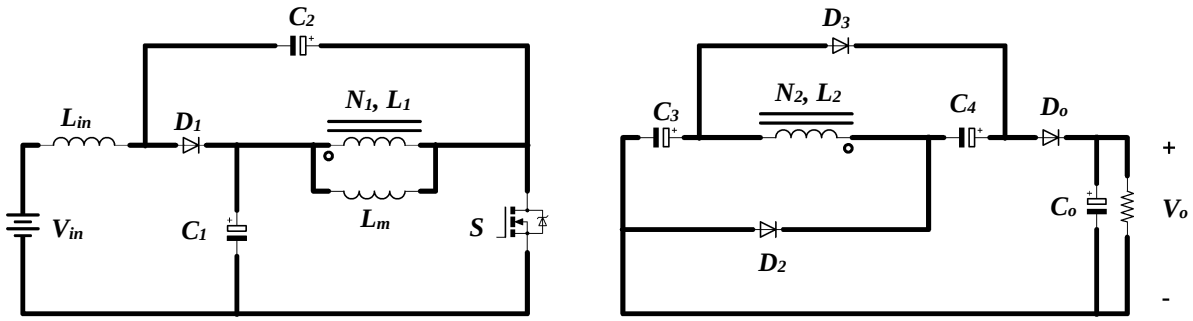

Figure 2. *The proposed converter*

Conversion ratio, the switching period and the duty cycle are $n=N_2/N_1$, T_s and $D=T_{on}/T_s$, respectively. When the switch is turned on, the following equations can be obtained:

$$v_{Lin}^{I} = V_{in} + V_{C2} \quad (1)$$

$$v_{L1}^{I} = V_{C1} \quad (2)$$

$$v_{Lm}^{I} = V_{C1} \quad (3)$$

$$v_{L2}^{I} = -nv_{Lm}^{I} = -nV_{C1} \quad (4)$$

$$V_O = V_{C3} + V_{C4} - v_{L2}^{I} \quad (5)$$

When the switch is turned off the following equations can be obtained:

$$v_{Lin}^{II} = V_{in} - V_{C1} \quad (6)$$

$$v_{L1}^{II} = -V_{C2} \quad (7)$$

$$V_{C3} = V_{C4} = v_{L2}^{II} \quad (8)$$

The following equations can be written by using volt-second balance relationship for each inductor

$$\int_0^{DT_s} v_{L1}^{I} dt + \int_{DT_s}^{T_s} v_{L1}^{II} dt = 0 \quad (9)$$

$$\int_0^{DT_s} v_{Lin}^{I} dt + \int_{DT_s}^{T_s} v_{Lin}^{II} dt = 0 \quad (10)$$

$$\int_0^{DT_s} v_{Lm}^{I} dt + \int_{DT_s}^{T_s} v_{Lm}^{II} dt = 0 \tag{11}$$

$$\int_0^{DT_s} v_{L2}^{I} dt + \int_{DT_s}^{T_s} v_{L2}^{II} dt = 0 \tag{12}$$

V_{C1} and V_{C2} can be obtained by inserting Eqs. 2 and 7 in Eq.9.

$$\frac{V_{C2}}{V_{C1}} = \frac{D}{(1-D)} \tag{13}$$

The relationship between V_{in} and V_{C1}, V_{C2} voltages are reached by using Eqs. 1 and 6 in Eq. 10.

$$V_{C1} = \frac{(1-D)V_{in}}{(1-2D)} \tag{14}$$

$$V_{C2} = \frac{DV_{in}}{(1-2D)} \tag{15}$$

The voltage on the switch S (v_{DS}) is.

$$v_{DS} = V_{C1} + V_{C2} = \frac{V_{in}}{1-2D} \tag{16}$$

If Eqs. 11 and 12 are used in Eqs.3 and 4 v_{Lm}^{II} and v_{L2}^{II} voltages during the off-state is found.

$$v_{Lm}^{II} = -\frac{D}{1-D} V_{C1} = -V_{C2} \tag{17}$$

$$v_{L2}^{II} = \frac{nD}{1-D} V_{C1} = nV_{C2} \tag{18}$$

The voltages across the C_3 and C_4 capacitors when the switch is OFF

$$V_{C3} = V_{C4} = v_{L2}^{II} = \frac{nD}{1-D} V_{C1} \tag{19}$$

Finally, the output voltage is found by Eqs. 4 and 19 in Eq.5.

$$V_o = \frac{1+D}{1-D} nV_{C1} = nV_{in} \frac{1+D}{1-2D} \tag{20}$$

The voltage gain of the converter is then

$$G_{CCM} = \frac{V_o}{V_{in}} = \frac{1+D}{1-2D} n \tag{21}$$

II. PV MODULE CHARACTERISTIC AND CONTROL DIAGRAM

The single diode equivalent circuit of a PV module is shown in Fig. 3. The current–voltage (*I-V*) characteristic equation of the PV module can be written as follows

$$I = I_{PH} - I_o\left(\exp^{\frac{q(V+IR_s)}{AN_skT}} - 1\right) - \frac{V+IR_s}{R_{sh}} \tag{22}$$

In Eq. 1, I is output current , V is the output voltage, I_{PH} is photon current under a given irradiance and temperature level, I_o is the reverse saturation current, q is electron charge, k is the Boltzmann constant, A is the ideal parameter, T is the working temperature (K), N_s is the number of solar cells in series, R_s is the series resistance, and R_{sh} is the shunt resistance. The reverse saturation current (I_o) of the PV module varies with temperature as follows:

$$I_o = I_{or}\left[\frac{T}{T_r}\right]^3\left(\exp^{\frac{qE_{GO}}{kT}(\frac{1}{T_r}-\frac{1}{T})}\right) \tag{23}$$

The generated current (I_{PH}) of the PV module varies with temperature and irradiance as follows:

$$I_{PH} = \frac{\lambda}{1000}\left(I_{PH(ref)} + K_I(T - T_{ref})\right) \tag{24}$$

where I_{or} is the reverse saturation current at T_r, T is the temperature of the PV panel (K), T_r is the reference temperature, E_{GO} is the band-gap energy of the semiconductor used in the PV panel, K_I is the short-circuit current temperature coefficient and λ is the irradiance in W/m^2, T_{ref} is reference temperature, $I_{PH(ref)}$ is the photo current at T_{ref}.

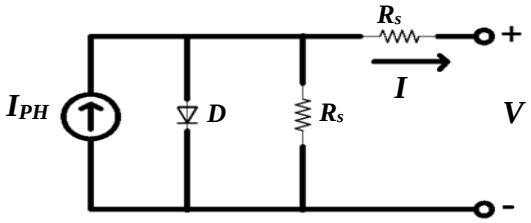

Figure 3*. The equivalent circuit of PV module*

The general control system model is depicted in Fig. 4. As seen from figure, the control system consists of a MPPT controller, a DC link voltage controller, and a current controller. The control system ensures the maximum available electrical power which is produced by the PV panel at any irradiance and temperature level to the grid with a unity power factor.

The MPPT controller maximizes generated power by PV under different weather conditions and solar radiations and delivers it to grid. Its output generates the reference peak current of the current controller. For implementing the MPPT algorithm, Perturb and observe method is used [24]. To keep the DC link voltage constant, PID controller is used. The output of the controller is a function of duty cycle for the *S* switch. A PI controller is implemented as the current controller for the application. The

output of the MPPT controller is multiplied by a synchronous signal sin(θ) with grid. This generates the reference current of the current controller. Grid current i_{grid} is sensed and then is compared to reference current $i_{rid(ref)}$. The error produced is fed to the PI controller. Finally, the output of the PI controller is compared to the triangular wave to produce the switching signals for the full bridge. The mathematical formulation of the PI algorithm is discussed in detail in [25].

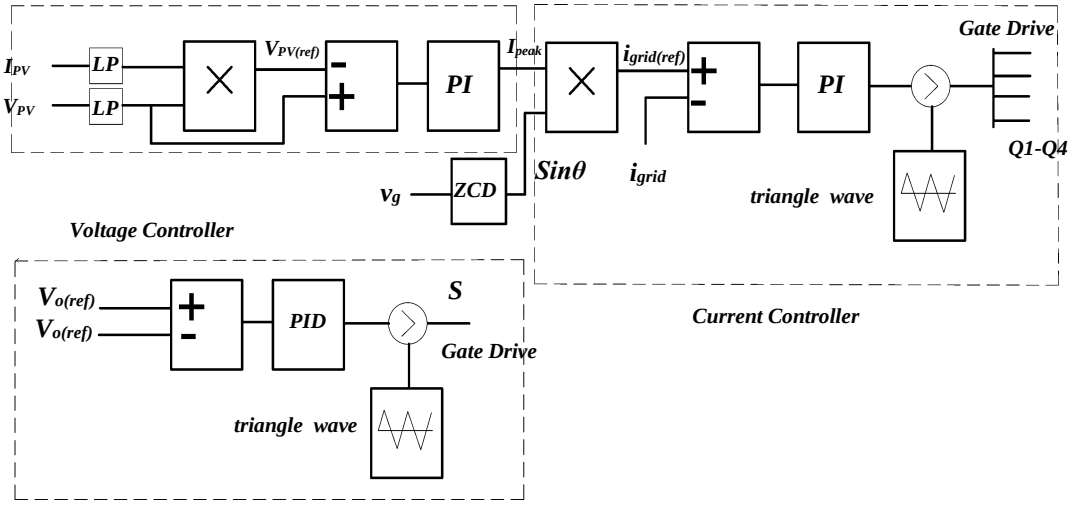

Figure 4. *Control block diagram*

III. SIMULATION RESULTS

The proposed configuration is simulated in MATLAB/Simulink. Table I shows the characteristics of the PV panel used in the simulation. The converter parameters are given in Table II. The ideality factor is one for the ideal diode. The PV panel which is to be used with this system consists of 52 solar cells and produces a 300 W of maximum power and a 32.3 *V* of open-circuit voltage at 1 kW/m^2 of an irradiance and 25 ^oC of a temperature. I-V and P-V curves of the PV panel in various irradiance and temperature levels are shown in Fig. 5.

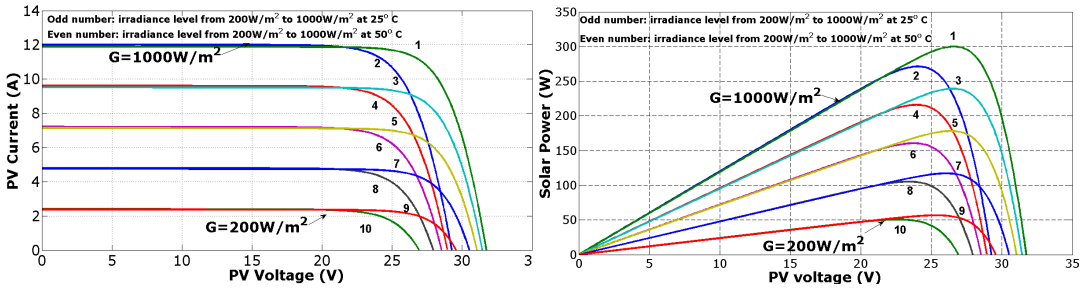

(a) (b)

Figure 5. *(a) I-V and (b) P-V characteristics of the PV module with varying temperature and irradiance*

The irradiance and temperature levels may change rapidly under atmospheric conditions. In view of this study, sudden step changes in various irradiance and temperature levels are applied to the simulation process. At *t*=0.1 *s* and 0.2 *s*, the irradiance level decreases from 1000 W/m^2 to 200 W/m^2 in

steps of 400 W/m^2. At t=0.3 s, the temperature level raises from 25 ^oC to 50 ^oC. Fig. 6 shows step changes.

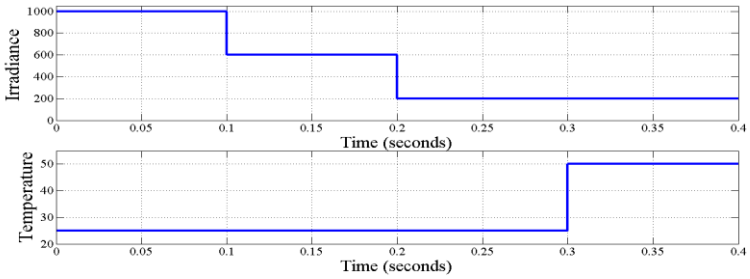

Figure. 6. *Sudden step changes in the irradiance and temperature levels.*

Table 1. *PV module characteristics*

Parameter	Value
Max Power	300 W
$I_{PH(ref)}$	11.9 A
I_{MPPT}	11.35 A
V_{MPPT}	26.45 V
k	1.38e^{-23}
q	1.602e^{-19}
R_s	0.1 Ω
R_{sh}	1000 Ω
N_s	52
E_{GO}	1.1 eV
I_{or}	1e^{-9} A
K_I	0.0047 $A/^oC$
T_r	*301.18 ^oK*
T_{ref}	*25 ^oC*

Table 2. *The converter parameters*

Parameter	Value
Grid Voltage	220 *V(rms)*
C_{in}	10 mF
C_1=C_2	0.82 mF
C_3=C_4	0.1 mF
C_o	2 mF
L_{in}	66 μH
L_f	10 mH
L_1	33 μH
L_2	465 μH

Fig. 7 shows the variation of PV module's output voltage, current, and power and Fig. 8 shows grid voltage and current. Till t=0.1 s, the irradiance and temperature levels are 1000 W/m^2 and 25 ºC, respectively. The power obtained from the PV module is about 300 W. When the irradiance level decreases, the output voltage of the PV panel decrease too. In this case, the MPPT algorithm reduces the duty cycle ratio for the switch S to increase the output voltage of PV module. Fig. 7 shows that the MPPT algorithm tracks the maximum available power of PV module. Fig. 8 shows that the full bridge inverter in the second stage delivers solar power to 220 $V_{(rms)}$ of the grid with a unity power factor.

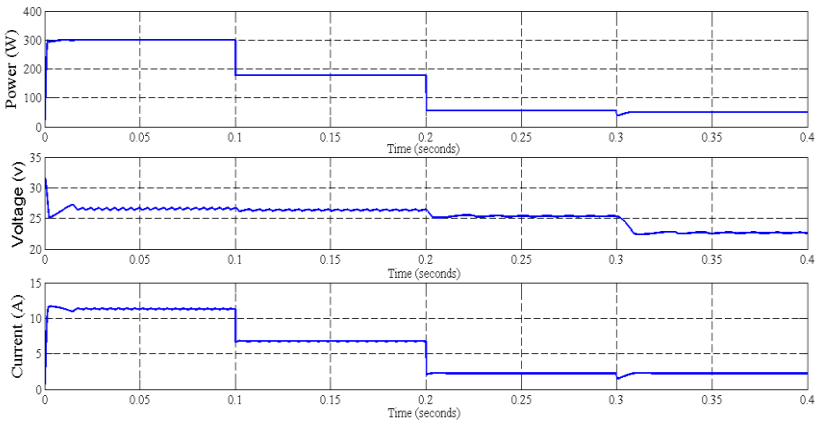

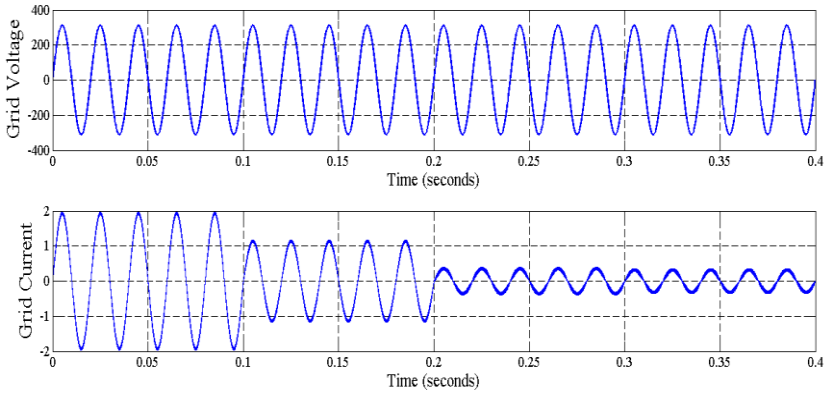

Figure 7*. The variation of PV module power, output voltage and current*

In this paper, solar based single phase grid connected inverter system is presented for AC module applications. The system is consists of a full-bridge inverter and s DC-DC converter. MATLAB-Simulink is used to simulate all system. Low THD and high power factor is obtained. High step-up DC–DC converters have large input currents for AC module applications. This increases conduction losses. Whereas, the proposed converter allows lower voltage-rated devices with small $R_{DS(on)}$ which is used to reduce conducting losses. This means efficiency increases.

IV. REFERENCES

[1] Kjaer, S.B.; Pedersen, J.K.; Blaabjerg, F.; , "A review of single-phase grid-connected inverters for photovoltaic modules," *Industry Applications, IEEE Transactions on* , vol.41, no.5, pp. 1292-1306, 2005.

[2] Yaosuo Xue; Liuchen Chang; Sren Baekhj Kjaer; Bordonau, J.; Shimizu, T.; , "Topologies of single-phase inverters for small distributed power generators: an overview," *Power Electronics, IEEE Transactions on* , vol.19, no.5, pp. 1305- 1314, 2004.

[3] Quan Li; Wolfs, P.; , "A Review of the Single Phase Photovoltaic Module Integrated Converter Topologies With Three Different DC Link Configurations," *Power Electronics, IEEE Transactions on* , vol.23, no.3, pp.1320-1333, 2008.

[4] Meneses, D.; Blaabjerg, F.; García, O.; A. Cobos, J.; , "Review and Comparison of Step-Up Transformerless Topologies for Photovoltaic AC-Module Application," *Power Electronics, IEEE Transactions on* , vol.28, no.6, pp.2649-2663, 2013.

[5] Jain, S.; Agarwal, V.; , "A Single-Stage Grid Connected Inverter Topology for Solar PV Systems With Maximum Power Point Tracking," *Power Electronics, IEEE Transactions on* , vol.22, no.5, pp.1928-1940, 2007.

[6] Yu Fang; Xudong Ma; , "A Novel PV Microinverter With Coupled Inductors and Double-Boost Topology," *Power Electronics, IEEE Transactions on* , vol.25, no.12, pp.3139-3147, 2010.

[7] Rahim, N.A.; Chaniago, K.; Selvaraj, J.; , "Single-Phase Seven-Level Grid-Connected Inverter for Photovoltaic System," *Industrial Electronics, IEEE Transactions on* , vol.58, no.6, pp.2435-2443, 2011.

[8] Wensong Yu; Jih-Sheng Lai; Hao Qian; Hutchens, C.; , "High-Efficiency MOSFET Inverter with H6-Type Configuration for Photovoltaic Nonisolated AC-Module Applications," *Power Electronics, IEEE Transactions on* , vol.26, no.4, pp.1253-1260, 2011.

[9] Zhou, Y.; Liu, L.; Li, H.; , "A High-Performance Photovoltaic Module-Integrated Converter (MIC) Based on Cascaded Quasi-Z-Source Inverters (qZSI) Using eGaN FETs," *Power Electronics, IEEE Transactions on* , vol.28, no.6, pp.2727-2738, 2013.

[10] Kwon, J.-M.; Kwon, B.-H.; Nam, K.-H.; , "High-efficiency module-integrated photovoltaic power conditioning system," *Power Electronics, IET* , vol.2, no.4, pp.410-420, 2009.

[11] Tan, G.H.; Wang, J.Z.; Ji, Y.C.; , "Soft-switching flyback inverter with enhanced power decoupling for photovoltaic applications," *Electric Power Applications, IET* , vol.1, no.2, pp.264-274, 2007.

[12] Nanakos, A.C.; Tatakis, E.C.; Papanikolaou, N.P.; , "A Weighted-Efficiency-Oriented Design Methodology of Flyback Inverter for AC Photovoltaic Modules," *Power Electronics, IEEE Transactions on* , vol.27, no.7, pp.3221-3233, 2012.

[13] Yanlin Li; Oruganti, R.; , "A Low Cost Flyback CCM Inverter for AC Module Application," *Power Electronics, IEEE Transactions on* , vol.27, no.3, pp.1295-1303, 2012.

[14] Kim, Y.-H.; Ji, Y.-H.; Kim, J.-G.; Jung, Y.-C.; Won, C.-Y.; , "A New Control Strategy for Improving Weighted Efficiency in Photovoltaic AC Module-Type Interleaved Flyback Inverters," *Power Electronics, IEEE Transactions on* , vol.28, no.6, pp.2688-2699, 2013.

[15] Hu, H.; Harb, S.; Kutkut, N. H.; Shen, Z. J.; Batarseh, I.; , "A Single-Stage Microinverter Without Using Eletrolytic Capacitors," *Power Electronics, IEEE Transactions on* , vol.28, no.6, pp.2677-2687, 2013.

[16] Huang-Jen Chiu; Yu-Kang Lo; Chun-Yu Yang; Shih-Jen Cheng; Chi-Ming Huang; Ching-Chun Chuang; Min-Chien Kuo; Yi-Ming Huang; Yuan-Bor Jean; Yung-Cheng Huang; , "A Module-Integrated Isolated Solar Microinverter," *Industrial Electronics, IEEE Transactions on* , vol.60, no.2, pp.781-788, 2013.

[17] S. Yatsuki, K. Wada, T. Shimizu, H. Takagi, and M. Ito, “A novel AC photovoltaic module system based on the impedance-admittance conversion theory,” in *Proc. IEEE PESC*, 2001, pp. 2191–2196.

[18] K. C. A. de Souza, M. R. de Castro, and F. Antunes, “A DC/AC converter for single-phase grid-connected photovoltaic systems,” in *Proc. IEEE IECON*, 2002, pp. 3268–3273.

[19] Kwon, J.-M.; Kwon, B.-H.; Nam, K.-H.; , "High-efficiency module-integrated photovoltaic power conditioning system," *Power Electronics, IET* , vol.2, no.4, pp.410-420, 2009.

[20] Ching-Tsai Pan; Ching-Ming Lai; Ming-Chieh Cheng; , "A Novel Integrated Single-Phase Inverter With Auxiliary Step-Up Circuit for Low-Voltage Alternative Energy Source Applications," *Power Electronics, IEEE Transactions on* , vol.25, no.9, pp.2234-2241, 2010.

[21] Fang Zheng Peng; , "Z-source inverter," *Industry Applications, IEEE Transactions on* , vol.39, no.2, pp. 504- 510, 2003.

[22] Anderson, J.; Peng, F.Z.; , "Four quasi-Z-Source inverters," *Power Electronics Specialists Conference, 2008. PESC 2008. IEEE* , pp.2743-2749, 2008.

[23] Wei Qian; Fang Zheng Peng; Honnyong Cha; , "Trans-Z-Source Inverters," *Power Electronics, IEEE Transactions on* , vol.26, no.12, pp.3453-3463, 2011.

[24] Esram, T.; Chapman, P.L.; , "Comparison of Photovoltaic Array Maximum Power Point Tracking Techniques," *Energy Conversion, IEEE Transactions on* , vol.22, no.2, pp.439-449, 2007.

[25] Kitano, T.; Matsui, M.; De-hong Xu; , "Power sensor-less MPPT control scheme utilizing power balance at DC link-system design to ensure stability and response," *Industrial Electronics Society, 2001. IECON '01. The 27th Annual Conference of the IEEE* , vol.2, pp. 1309-1314, 2001.